Journal of Coastal Research	00	0	000–000	Coconut Creek, Florida	Month 0000

Coseismic Subsidence and Paleotsunami Run-Up Records from Latest Holocene Deposits in the Waatch Valley, Neah Bay, Northwest Washington, U.S.A.: Links to Great Earthquakes in the Northern Cascadia Margin

www.cerf-jcr.org

Curt D. Peterson[†], Kenneth M. Cruikshank[†], Mark E. Darienzo[†], Gary C. Wessen[‡], Virginia L. Butler[§], and Sarah L. Sterling[§]

[†]Geology Department
Portland State University
Portland, OR 97207-0751, U.S.A.
petersonc@pdx.edu

[‡]Wessen and Associates
15028 24th Avenue SW
Seattle, WA 98166, U.S.A.

[§]Anthoplology Department
Portland State University
Portland, OR 97207-0751, U.S.A.

www.JCRonline.org

ABSTRACT

Peterson, C.D.; Cruikshank, K.M.; Darienzo, M.E.; Wessen, G.C.; Butler, V.L., and Sterling, S.L., 0000. Coseismic subsidence and paleotsunami run-up records from latest Holocene deposits in the Waatch Valley, Neah Bay, northwest Washington, U.S.A.: links to great earthquakes in the northern Cascadia Margin. *Journal of Coastal Research,* 00(0), 000–000. Coconut Creek (Florida), ISSN 0749-0208.

Representative shallow cores (1–2-m depth) from the Waatch Valley ($n = 10$) and from Neah Bay back-barrier wetlands ($n = 7$) record four coseismic subsidence events and associated paleotsunami inundations during the last 1300 years in the North Central Cascadia Margin. Three of the subsidence events (SUB1, SUB2b, and SUB3) correlate to reported great earthquakes dated at AD 1700, about 1.1 ka, and about 1.3 ka. An additional subsidence horizon (SUB2a), which is newly discovered in the study area, might correlate to a widely reported paleotsunami inundation, dated between 0.7 and 0.9 ka in the study region. The magnitudes of paleosubsidence in the Waatch Valley are modest (about 0.5–1.0 m), as based on macofossil evidence of abrupt wetland burial. Paleotsunami origins of the four landward thinning sand sheets are confirmed by the presence of ocean diatom taxa and beach sand grains. Long wave run-up in the low-gradient Waatch floodplain ranged from 2.5 to 4.5 km up-valley distance from the present tidal inlet shoreline. Paleotsunami overtopping of the Neah Bay barrier ridge (6–8-m elevation North American Vertical Datum of 1988 [NAVD88]) provides the first estimates of paleotsunami minimum run-up height at the entrance to the Juan de Fuca Strait.

ADDITIONAL INDEX WORDS: *Tsunami, subsidence, earthquakes, subduction zone, diatoms, radiocarbon.*

INTRODUCTION

In this study we report on the geologic records of basin sedimentation, episodic subsidence, and tsunami run-up in latest Holocene wetland deposits of the Waatch Valley, located near Neah Bay, Washington (Figure 1). The relatively young marsh deposits in the Waatch Valley host records of great earthquake coseismic subsidence and nearfield tsunami run-up that occurred in the northernmost end of the North Central Cascadia Margin. The narrow Waatch Valley contains the only tidal marshes that could host such records on the west coast of northern Washington.

Broad tidal marshes in Willapa Bay, located south of the study area (Figure 1), yield extensive records of episodic coseismic subsidence in the southern part of the North Central Cascadia Margin (Atwater *et al.,* 2004). However, back-edge marshes in the large Willapa Bay embayment do not reliably record tsunami inundations. Tidal marshes also occur in fjord embayments along the west coast of Vancouver Island, such as at Tofino, British Columbia. However, postglacial isostatic uplift of the west coast of Vancouver Island has limited the marsh subsidence records to the last Cascadia megathrust rupture at AD 1700 (Clague and Bobrowsky, 1994a). Paleotsunami deposit records are reported from Discovery Bay, Washington, located east of Neah Bay in the Juan de Fuca Strait (Williams, Hutchinson, and Nelson, 2005). A lack of associated coseismic subsidence records in Discovery Bay precludes drawing a direct connection between the preserved paleotsunami sand sheets and Cascadia megathrust ruptures. This leads to the question: are the Discovery Bay sand sheets the products of Cascadia tsunamis that propagated into the Juan de Fuca Strait or are they from other sources, such as local faults, landslides, or underwater slumps?

Before our study, Atwater (1992) conducted a reconnaissance study of the Waatch Valley wetlands to search for evidence of cyclic coseismic coastal subsidence. Only one marsh burial event was observed in the middle reaches of the Waatch Valley. The origin of this subsidence event was unclear as five radiocarbon ages on associated organics returned about a 750-year spread (795-1263) (Atwater, 1992). Paleotsunami

DOI: 10.2112/JCOASTRES-D-12-00031.1 received 15 February 2012; accepted in revision April 12, 2012.
Published Pre-print online 21 August 2012.
© Coastal Education & Research Foundation 2012

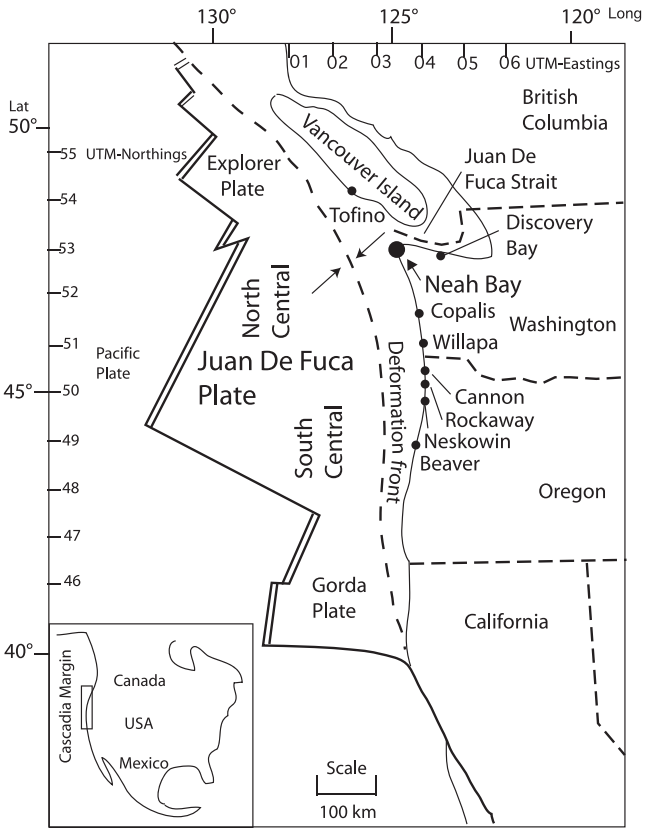

Figure 1. Location map showing the position of Neah Bay and several localities (black circles) with evidence for great earthquake or paleotsunami records (or both) in the Cascadia Margin. The position of the deformation front, or buried trench (dashed line), is shown about 140 km offshore (west) of Neah Bay. Convergence (opposing arrows) between the North American Plate (mainland and Vancouver Island) and the subducting oceanic plate (Juan de Fuca Plate) results in episodic megathrust rupture and associated near-field tsunami excitation. Map coordinates are in degrees longitude and latitude and meters UTM easting and northing.

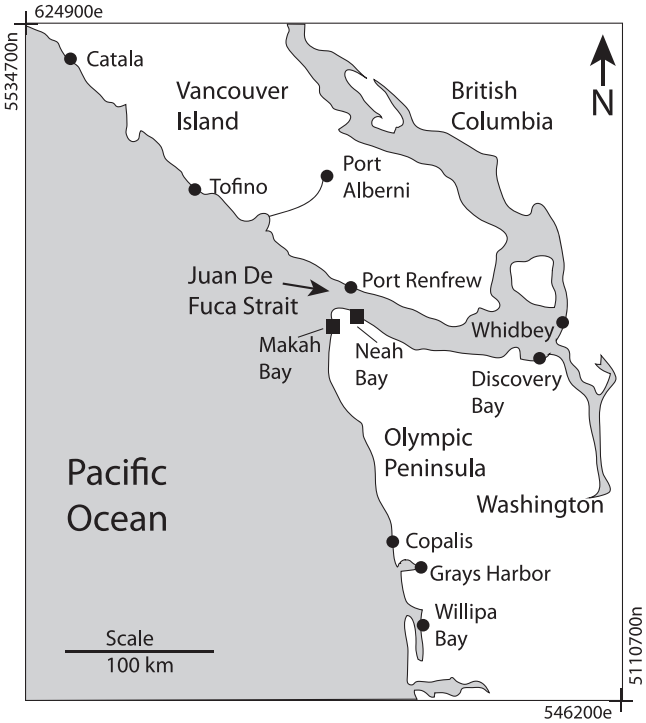

Figure 2. Localities (black circles) reported to contain records of coseismic subsidence or tsunami surge deposition (or both). See Clague, Bobrowsky, and Hutchinson (2000) for additional inferred paleotsunami sites on the west coast of Vancouver Island. The Waatch Valley extends between Makah Bay and Neah Bay (black squares) at the northwest end of the Olympic Peninsula. Map coordinates are in meters UTM easting and northing. See Table 1 for summarized coseismic subsidence or paleotsunami data.

sand sheets were not reported for the lower Waatch Valley floodplain.

More extensive investigations of the middle and upper Waatch Valley wetlands were undertaken by these investigators to establish (1) the latest Holocene records of relative sea-level rise and net sedimentation, (2) cyclic coseismic marsh subsidence, and (3) near-field paleotsunami run-up height. The Waatch Valley was investigated in this study for modern conditions of salinity, vegetation, and microfossil indicators of tidal level and marine water inundation. Shallow coring was performed to establish subsurface records of net sedimentation, habitat change, coseismic subsidence or uplift, and paleotsunami inundations.

Plant macrofossil evidence from shallow cores throughout the Waatch Valley demonstrates several events of abrupt marsh submergence with associated anomalous sand deposition. Ocean diatom microfossils establish that the sand sheets originated from catastrophic marine surge, superimposed on longer records of infilling of the Waatch Valley. Radiocarbon dates and event sequence link the submergence and marine surge inundation events to regional great earthquakes and tsunami excitation in the northernmost end of the North Central Cascadia Margin (Figure 1).

BACKGROUND

The longest record of coseismic subsidence events in the North Central Cascadia Margin (Figure 2) is reported from Willapa Bay, Washington (Table 1), where at least seven events occurred in 3200 years (Atwater *et al.,* 2004). The greatest number of apparent paleotsunami events (seven to nine events in 2700 years) is reported from Discovery Bay, Washington (Williams, Hutchinson, and Nelson, 2005). For this study we focus on the last 1500 years of paleoseismic evidence in the northern Cascadia region, which is about the age limit of the Waatch wetlands (see "Results" below). Three paleotsunami sand layers are reported from the coastal Catala Lake during the last 1500 years on the west coast of Vancouver Island. The paleotsunami records are not well developed in Willapa Bay and no coseismic subsidence events are recorded at Discovery Bay, or the nearby Whidbey Island locality.

Table 1. *Summary of coastal subsidence and paleotsunami records during the last 1500 years in the study region.*

Locality	Event TSL/Sub	RC Age Adjusted	Calibrated AD/y BP/ka	Overland Run-Up Dist. (m)/Ht. (m)	Ref.
Catala	TSL/	460 ± 80‡	AD 1700	500/5 MSL	1
	TSL/	1000 ± 60	778-1055	500/5 MSL	1
	TSL/	1300 ± 70‡	1063–1330	500/5 MSL	1
Tofino	TSL*/	<180	AD 1964?	50/2 MSL	2
	TSL†/Sub	440 ± 60‡	AD 1700	100/2 MSL	
	TSL	680 ± 50	510–780	100/1.6 MSL	
Port Alberni	TSL		AD 1964	300/1.3 MSL	3
	TSL	270 ± 60	AD 1700	300/1.1 MSL	
	TSL	880 ± 90	670–954	300/0.7 MSL	
	TSL	1160 ± 90	930-1273	300/0.4 MSL	
	TSL	1280 ± 70	1014–1311	50/0.0 MSL	
Port Renfrew	TSL/Sub?		AD1700	na	4
Whidbey	TSL*/	1330 ± 50	1160–1350	100/3.0	5
	TSL*/	1630 ± 50	1400–1700	100/3.0	
Discovery	TSLlaminae/	AD 1964		250/3.4	6
	TSL^{C}/		0–295	250/3.4	
	TSL/		300–500	130/3.2	
	TSL/		1130–1260	86/2.9	
	TSLthick/		960–1270	86/2.8	
	TSLlaminae?/		1140–1300	20/2.6	
	TSL		1560–1820	86/2.2	
Copalis	TSL*/Sub	230 ± 45	AD 1700	1200/1.0	7
	/Sub?	1050 ± 100	739-1221		
		1720 ± 70	1419–1820		
	TSL*/Sub	1673 ± 80	1391–1810	1500/0.5	
Willapa	TSL*/Sub–Y		AD 1700	100/3.4	8
	/Sub–W		1.1 ka		
	/Sub–U		1.3 ka		
	/Sub–S		1.7 ka		

The Catala core sites are in a coastal lake, with a current elevation of 5 m above present sea level (Figure 2). The Tofino core sites are in tidal marshes. The Port Alberni core sites are in a supratidal delta plain at the head of a fjord. The Discovery Bay and Whidbey core sites are in tidal marshes adjacent to the Juan De Fuca Strait. The Copalis core sites are in tidal creek marshes. The Willapa Bay core sites are from the Niawiakum tidal creek marshes at the eastern edge of the broad Willapa tidal basin.

* Linked to Cascadia rupture event.

† Not linked to Cascadia rupture event.

‡ Middle date of three to four clustered radiocarbon dates.

Radiocarbon dates (RC) include both isotope and adjusted dates and calibrated dates. Radiocarbon date calibrations (2 σ) for Catala, Tofino, and Copalis are from CALIB v6.0html (Stuiver, Reimer and Reimer, 2011). Previous calibrations of the Copalis dates are presented in a microfiche table (Atwater, 1992). All other date calibrations are as originally published.

Run-up distance: Dist. (m) is overland distance from shoreline.

Run-up height: Ht. (m) is elevation relative to the North American Vertical Datum of 1988 (NAVD88) or to mean sea level (MSL). NAVD88 is about 1.0 m below NGVD29 or MSL in the study area.

References: (1) Clague *et al*. (1999), (2) Clague and Bobrowsky (1994a), (3) Clague and Bobrowsky (1994b), (4) Clague, Bobrowsky, and Hutchinson (2000), (5) Williams and Hutchinson, 1998 (6) Williams, Hutchinson, and Nelson (2005), (7) Atwater (1992), (8) Atwater et al. (2004).

The only direct linkage between dated coseismic subsidence and paleotsunami run-up in the northernmost Cascadia Margin is at Tofino in Vancouver Island (Figure 2). Slowing of postglacial rebound permitted the development of tidal marshes in the west coast of Vancouver Island within the last 500 years (Clague and Bobrowsky, 1994a). An abrupt marsh submergence and associated near-field tsunami inundation in Tofino are correlated to the last Cascadia megathrust rupture at AD 1700 (Table 1). An older paleotsunami sand sheet (500–780 BP) occurs in a shallow tidal flat mud in Tofino, but it, along with deeper sand layers in the bay muds, cannot be directly linked to local records of coseismic subsidence (Clague, Bobrowsky, and Hutchinson, 2000). A possible minor subsidence record is reported to be associated with the AD 1700 Cascadia paleotsunami at Port Renfrew, near the head of Botany Bay in the southwest coast of Vancouver Island (Clague, Bobrowsky, and Hutchinson, 2000), but details of its extent are not provided.

The next locality to the south of Vancouver Island that includes a reported record of coseismic subsidence and associated near-field paleotsunami inundation is at Copalis, Washington (Atwater, 1992). Only two inferred great earthquakes are dated in Copalis, at AD 1700 and at 1419–1820 BP (Table1). Paleoliquefaction features obscure other paleoseismic records at about 1000 years BP in some of the Copalis River cutbank exposures (Atwater, 1992). The Waatch Valley is positioned between the coastal subsidence sites at Tofino, British Columbia and Copalis, Washington and the paleotsunami record site in Discovery Bay, Washington (Figure 2).

The narrow Waatch Valley extends between Makah Bay in the Pacific Ocean and Neah Bay in the Juan de Fuca Strait. The Waatch Valley wetlands are especially well suited for tracking paleotsunami inundations from both the Pacific Ocean and

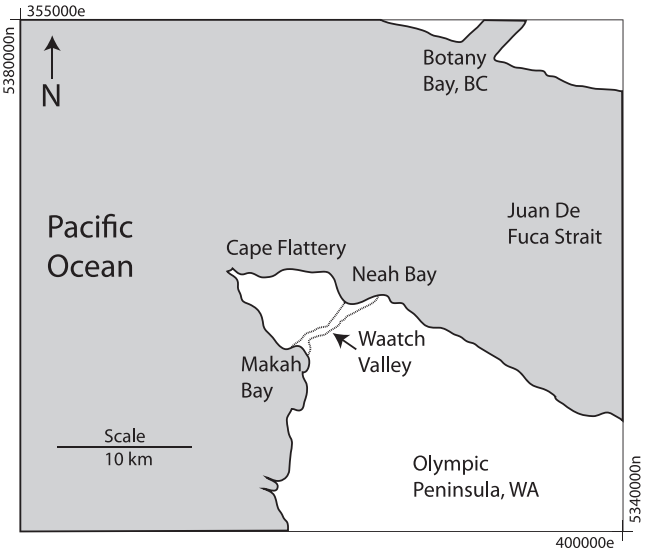

Figure 3. Study area map showing the Waatch Valley between Makah Bay in the Pacific Ocean coast and Neah Bay in the Juan de Fuca Strait. The spelling of Waatch is the anglicized form of a Makah Tribe place name, as known from multiple spellings. The Waatch spelling conforms to its use in U.S. Geological Survey maps. Map coordinates are in meters UTM easting and northing.

Juan de Fuca Strait (Figure 3). The marsh deposits in the Waatch Valley could provide the only direct linkages between cyclic or multiple events of coastal subsidence and paleotsunami excitation in the northern end of the North Central Cascadia Margin (see "Introduction"). The Waatch Valley wetlands are characterized by two other unique conditions of (1) an extensive low-gradient alluvial plain (about 3.0-m rise over 5-km distance) connected to the Pacific Ocean and (2) a beach barrier dune ridge (6–8 m in elevation) located at the entrance of the Juan de Fuca Strait (Figure 3). These conditions provide the potential for finding records of paleotsunami inundation distance and run-up height, both on the open coast and in the Juan de Fuca Strait.

METHODS

Elevation controls for channel salinity stations (S1–S3) and shallow core sites are provided by the National Oceanic and Atmospheric Administration (NOAA)-installed global positioning system (GPS) benchmarks (E1–E4) using OPUS-GEOID09 and EDM 1″ Theodolite Total Station surveys (combined vertical resolution ± 0.1 m North American Vertical Datum of 1988 [NAVD88]) (Figure 4). The NAVD88 datum is about 1 m below the older National Geodetic Vertical Datum of 1929 datum and mean sea level (MSL) in the study area. Wetland surface elevations range from about 1.5 m to 4.5 m NAVD88 with distance landward from the Pacific Ocean in the 5-km-long Waatch Valley. The maximum elevation of the Neah Bay barrier dune ridge at E1 is 9 m (Table 2). Tidal range in the study area is about ±1.5 m MSL. Annual rainfall is about 250 cm y^{-1}.

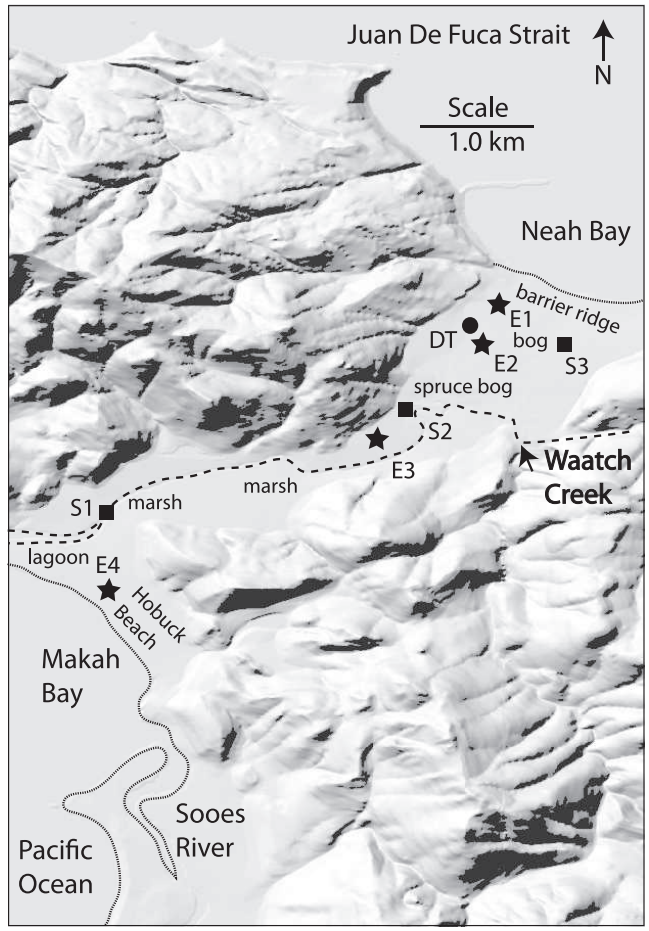

Figure 4. Hill-shaded digital elevation model (DEM) of Waatch Valley, including the Waatch Creek channel (dashed line), NOAA GPS elevation benchmarks (stars E1–E4), channel salinity stations (squares S1–S3), vegetation zonation (marsh and spruce bog), and clustered modern diatom sample stations (DT) at core sites W06 and W12 (see Figure 5 for numbered core sites). DEM background image is from U.S. Geological Survey (2011).

Vegetation surveys and surface diatom samples in the Waatch wetlands were collected at core sites with measured elevation in the Waatch Valley (Table 2). Salinity was measured with a conductivity probe in the Waatch Channel (S1), flooded marsh adjacent to the channel (S2), and flooded back-barrier bogs (S3) during a very high tide (3.0 m; February 2, 2011). Modern diatom samples were collected from three surface deposits each from two core sites (W06 and W12) in the upper Waatch Valley wetlands to test for the presence of full marine or ocean diatoms transported inland by windblown ocean spray (Peterson *et al.,* 2010). Diatom preparation follows Darienzo (1991) and Schlichting (2000). Both qualitative and quantitative species counts were performed on largely intact diatom valves in piccolyte mounts using total slide counts under 600× microscopy. Species taxonomy identifications are based on Hemphill-Haley (1993), Jensen and Hustedt (1985), and Patrick and Reimer (1966).

Table 2. *Elevations and position coordinates of GPS benchmarks, salinity stations, and core sites in Waatch Valley and Neah Bay back-barrier wetlands.*

Station/site	Setting	Lat./UMTe (m)	Long./UTMn (m)	Elev. (m)
NOAA GPS BM				
E1 GPS BBCJ12	Barrier ridge intersection	48°22′04.5012″/379423.63	−124°37′40.9344″/5358474.54	8.96
E2 GPS BBCJ14	Upper Valley Road	48°21′41.3246″/379322.09	−124°37′45.1307″/5357760.81	6.32
E3 GPS BBCJ15	Lower Valley Road	48°21′11.9112″/378565.07	−124°38′20.9803″/5356868.42	4.98
E4 GPS BBCJ13	Hobuck Beach ridge	48°20′21.7872″/376590.91	−124°39′55.2816″/5355362.71	6.25
Channel salinity				
S1 HB Bridge	Waatch lower reaches	48°20′50″/376800	−124°39′50″/5356210	2.5
S2 Site009	Waatch middle reaches	48°21′20″/378870	−124°38′10″/5357160	3.5
S3 Backtrack	Waatch back-barrier	48°21′40″/380000	−124°37′10″/5357840	4.0
Waatch core sites				
W14	Marsh	48°20′50″/376960	−124°39′40″/5356130	2.5
W01	Marsh	48°21′00″/377590	−124°39′10″/5356530	–
W02	Marsh	48°20′50″/377610	−124°39′10″/5356400	–
W03	Marsh	48°21′10″/378640	−124°38′20″/5356820	2.9
W04	Marsh	48°21′10″/378690	−124°38′10″/5356730	2.7
WA–M cutbank		–	–	
W13	Spruce bog	48°21′32″/379200/	−124°37′50″/5357490	3.3
W09	Spruce bog	48°21′40″/379260	−124°37′50″/5357680	3.9
W11	Spruce bog	48°21′40″/379600	−124°37′30″/5357650	–
W12	Spruce bog	48°21′40″/379240	−124°37′50″/5357810	3.8
W06	Spruce bog	48°21′50″/379270	−124°37′50″/5357920	–
Neah core sites				
N07	Back-barrier bog	48°22′00″/379360	−124°37′40″5358350	4.5*
N8a	Back-barrier bog	48°21′50″/379330	−124°37′40″/5358210	4.4*
N8b	Back-barrier bog	48°22′00″/379330	−124°37′40″/5358280	4.5*
N17	Back-barrier bog	48°21′50″/379390	−124°37′40″/5358170	4.5
CEM01	Dune ridge crest	–	–	
N18	Back-barrier bog	48°21′50″/380220	−124°37′00″/5358090	4.5
N20	Back-barrier bog	48°21′50″/380360	−124°36′50″/5357980	4.0
N19	Back-barrier bog	48°21′50″/380330	−124°36′50″/5357960	3.5

GPS coordinates are meters UTM easting and northing (NAD83 horizontal datum), and meters elevation (NAVD88 vertical datum).
Waatch wetland core sites (W01–W14 and N08a and N08b) are surveyed for elevation using EDT Total Station surveys from NOAA GPS base station benchmarks (E1–E4).
NOAA National Geodetic Survey Datasheets:
E1:http://www.ngs.noaa.gov/OPUS/getDatasheet.jsp?PID=BBCJ12 E2:http://www.ngs.noaa.gov/OPUS/getDatasheet.jsp?PID=BBCJ14
E3: http://www.ngs.noaa.gov/OPUS/getDatasheet.jsp?PID=BBCJ15
E4: http://www.ngs.noaa.gov/OPUS/getDatasheet.jsp?PID=BBCJ13
* Pasture fill is 20-cm thick in N08a, N08b, and N07.
Back-barrier core site elevations (N17, CEM01, N18, N20) are interpolated from 2′ (0.6 m) contour map: scale 1 : 1200 (Makah Indian Reservation, 1970) and 2′ contour map with photogrammetric control survey points (0.1 foot elevation): scale 1 : 600 (Makah Agency, 1972).

Subsurface Coring and Core Sample Analyses

Shallow coring (about 2-m subsurface depth) was performed with a 2.54-cm-diameter gouge core in continuous 1.0-m increments to refusal in basal sand deposits. Cores were photographed with a 15-mega pixel, digital single-lens reflex camera with 50-mm macrolens, and logged for lithology and plant macrofossil content. Selected cores were subsampled for diatoms, tsunami sand grain size, and radiocarbon samples. Sand layers and fining-upward trends in target paleotsunami layers are established with scaled high-resolution digital photos. Quantitative analyses of quartz and feldspar grain size distributions (wet sieved 0.0625–2.0-mm diameter) in paleotsunami sand layer intervals are based on 100 counts of grain intermediate diameters (D_i) per grain mount with micrometer under 250× microscopy. Radiocarbon samples were subsampled in the field and handpicked under binocular microscopy to reduce descending rootlets in the lab. All radiocarbon samples were submitted to Beta Analytic Inc. for accelerator mass spectrometry (AMS) dating. Radiocarbon results are presented in isotope-adjusted and calibrated 1-σand 2-σ ages (Stuiver, Reimer, and Reimer, 2011).

RESULTS

Modern Salinity, Vegetation, and Diatom Indicators

Modern salinity measurements in the Waatch Valley were taken at winter high tide (3.0 m), which together with Waatch Creek discharge and side slope runoff represent the conditions of maximum wetland flooding. Measured salinity decreases from brackish at S1 (about 2.5-m elevation, 1.2-km distance upriver) to fresh at S2 (3.5-m elevation, 3.5-km distance upriver) (Table 3). The back-barrier wetlands are fully freshwater at S3 (4.0-m elevation, 5.0-km distance upriver). Vegetation in wetland surfaces follows the salinity trends with *Distichlis* and *Salicornia* in low marsh settings at W14a,b (2.5-m elevation, 1.3-km distance upriver), *Potentilla* and *Deschampsia* at W03 (2.9-m elevation, 2.9-km distance upriver), and dense *Picea sitchensis* (Sitka spruce bog) at W09 (3.9-m

Table 3. *Modern salinity, vegetation, and diatom data from the Waatch Channel and Neah Bay back-barrier wetlands.*

Station	River Dist. (km)	Elev. (m)	Salinity (ppt)	Vegetation	Diatoms
S1	1.2	2.5	22.47		
W14a,b top channel	1.3	2.5		*Distichlis, Salicornia*	
	1.3	1.3		Lowest *Triglochin*	
W03 top channel	3.2	2.9		*Potentilla, Deschampsia*	
	3.2	1.5		Lowest vegetation	
S2	3.7	3.0	0.02		
W13	4.0	3.3		*Picea sitchensis* bog	
W09 top	4.4	3.9		*Picea sitchensis* bog	
W12 top	4.5	3.8		*Picea sitchensis* bog	Freshwater
W06	4.6	3.8			Freshwater
S3	5.0	4.0	0.03		

Modern channel salinity (S1–3) data collected February 2, 2011 at high tide (about 3.0 m NAVD88). See Figure 4 for positions of salinity stations, modern plant surveys, and modern diatom samples from the surface (top) of core sites (W09 and W12). Sloping channel banks (channel) demonstrate the lower limit of vegetation.
Elevation: Elev. is in meters NAVD88.
Salinity is in parts per thousand (ppt) as converted from conductivity.
Vegetation is characterized by salinity and flooding sensitive indicators of substrate organic content and specific plants including (1) rooted mud or colonizing marsh (*Triglochin*); (2) peaty mud or low marsh (*Distichlis* and *Salicornia*); (3) muddy peat or high marsh (*Potentilla* and *Deschampsia*); and (4) peat (>50% organics or tree roots) or supratidal bog (Sitka spruce).

elevation, 4.4-km distance upriver) (Figure 5). The transition between barren mud and colonizing marsh (*Triglochin*) is measured in channel accretionary banks across from W14b (1.3-m elevation, 1.3-km distance up-valley) and across from W03 (1.5-m elevation, 3.2-km distance up-valley).

Surface Sample Diatoms

Freshwater diatoms dominate the modern marsh surfaces in two partially diked wetland sites WA06 and WA12 (Table 4). Five of the six surface samples are dominated by freshwater oligohalobous diatoms. Four of the six sample analyses include only freshwater diatoms, which are consistent with the supratidal elevations (3.8–4.0 m NAVD88) and Sitka spruce bog vegetation at the sample locations. With a single exception of one sample from W12, windblown ocean diatoms in the polyhalobous group are not evident in the uppermost reaches of the Waatch Valley. A substantial presence of ocean water diatoms in the prehistoric Waatch Valley wetlands should be indicative of marine inundation by tides or other marine surge events, but not from ocean spray at this locality.

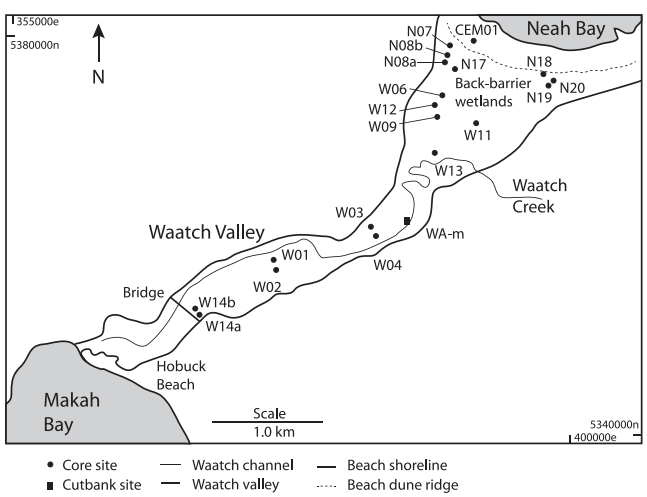

Figure 5. Core sites (numbered black circles) in Waatch Valley between Makah Bay in the Pacific Ocean and Neah Bay in the Juan de Fuca Strait. Core sites in the Waatch Valley floodplain are labeled (W). A subset of sites from the back-barrier wetlands in the northernmost Waatch Valley are labeled (N).

Waatch Valley Subsurface Core Data

To illustrate the general stratigraphy of the Waatch Valley wetlands a total of 10 representative cores is provided, showing 1–2 m of rooted mud and peaty mud, which overlie channel sand deposits (Figure 6). The medium-sized channel sand is subangular and moderately well sorted, though it contains rare fine gravel clasts. The channel sand fines up-core to muddy sand and then to overlying rooted mud, peaty mud, or muddy peat. The overlying mud sections generally thicken from 0.5 to 1.0 m at core sites W14a/b to 1.5 to 2.0 m at sites W13 and W09, W11, and W12, with increasing distance (1–4 km) landward in the Waatch alluvial floodplain. Mud sections in the middle and lower Waatch Valley thicken with increasing distance away from the central axis of the valley. In the center of the valley, such as at site W02, abandoned channel levees indicate recent migrations of the Waatch tidal channel. Shallow cores are used rather than cutbank exposures in this study to target valley sides, such as site W01, and upper Waatch Valley reaches, such as at W13–W12, where rooted mud and peaty mud deposits reach maximum thickness in the alluvial floodplain.

The mud deposits in the Waatch Valley wetlands vary in organic content, ranging from rooted mud (<5% organics) to peat (>50% organics or presence of tree roots). Abrupt contacts (<1-cm thickness) between underlying peaty mud or muddy peat and overlying rooted mud represent events of abrupt submergence. Cyclic events of low or high marsh burial by lower intertidal muds or colonizing marsh represent episodic coseismic subsidence (SUB). Seven of the 10 core sites in the Waatch Valley demonstrate multiple events of coseismic subsidence (Figure 6). Four coseismic strain cycles

Table 4. *Summary of diatoms from replicate surface samples at two partially diked sites WA06 and WA12 in the Waatch wetlands.*

Core Site	Sample #	Diatom Abundance	Diatom Trend (Slide Scan)
WA 06	1	Few	O
WA 06	2	Few	O
WA 06	3	Few	O
WA 12	1	Several	O–M
WA 12	2	Rare	O/P
WA 12	3	Rare	O

Key: P = polyhalobous, >30% salinity, includes "marine species"; M = mesohalobous, 0.2–30% salinity, includes "brackish species"; O = oligohalobous, <0.2% salinity, includes "freshwater species".
Dominance: X–YX is dominant; X/YX and Y are codominant. Species in polyhalobous, mesohalobous, and oligohalobous salinity tolerance ranges are listed in Appendix 1.
Core site positions are shown in Table 2 and Figure 5.

or marsh burial events (SUB1–4) are recorded at sites W13 and W06. Only one buried marsh horizon is identified in a previously reported and radiocarbon-dated core site WA–M (Atwater. 1992). Three subsidence events each are recorded at W01, W09, W11, and W12. The youngest subsidence event (SUB1) is relatively weakly developed in the Waatch Valley, not being distinguished in W01, WA–M, W11, and W12. However, it is well developed in some sites, such as W09, in the upper reaches of the Waatch Valley (Figure 7). The second subsidence event (SUB2) in the lower Waatch Valley is resolved into two very closely spaced subsidence events (SUB2a and SUB2b) in upper Waatch Valley at core sites W13, W09, W11, W12, and W06.

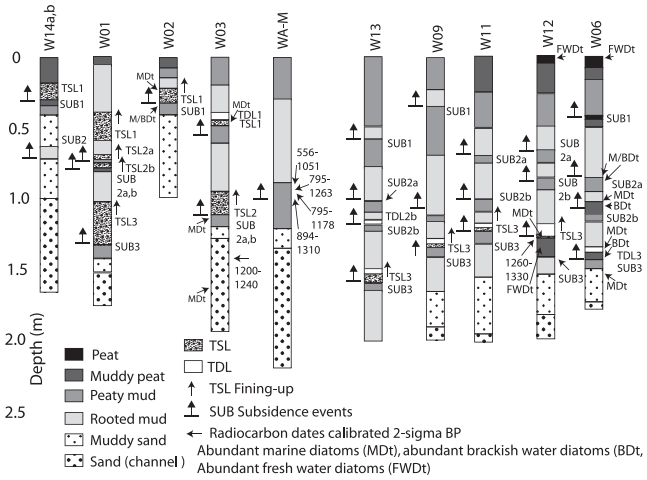

Figure 6. Summarized core logs from the Waatch Valley, ordered from the lower reaches (figure left) to the upper reaches (figure right). Paleosubsidence (SUB) contacts are locally overlain by paleotsunami sand layers (TSL) or paleotsunami debris layers (TDL). See Figure 5 for core site locations. Relative trends in diatom salinity indicators are shown for mostly marine diatoms (MDt), mostly brackish diatoms (BDt), or mostly freshwater diatoms (FWDt).

Diatom Salinity Indicators

Preliminary total slide counts for diatoms were conducted on selected subsurface samples from core site W06 in the upper Waatch Valley to test for any down-core changes in the relative abundances of marine, brackish, and freshwater diatoms (Figure 5). Sample intervals were selected to test for increased abundances of marine diatoms (polyhalobous) below the modern peat bog (see Table 4) and across coseismic subsidence or target paleotsunami layer contacts at 73–74-cm and 138–139-cm depth (Appendix 1). Observed increases in marine diatom abundances with increasing depth, generally, and across the specific event contacts at 73–74- and 138–139-cm depth, justified additional total slide count analyses to establish (1) long-term trends of tidal flow influence and (2) catastrophic marine surge inundation, respectively.

Diatom trend analyses were conducted on samples from basal sand deposits in W03 and W06 to test for marine tidal inundation conditions in the Waatch Valley before the

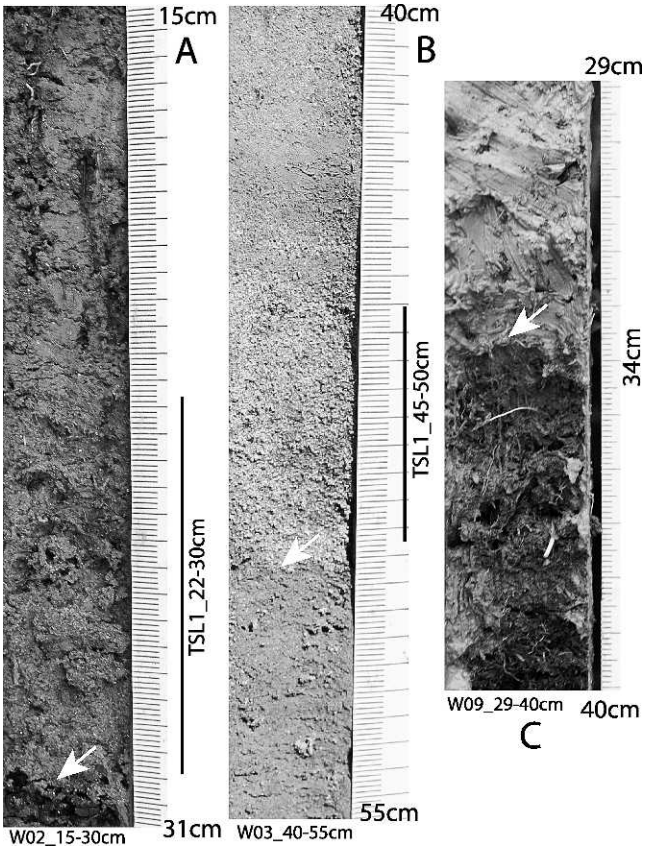

Figure 7. Core photographs of subsidence horizons (SUB1) and associated paleotsunami sand layers (TSL1 solid line) from the first coseismic subsidence event (AD 1700) in three Waatch Valley core sites. Scale tick marks are in millimeters. Subsidence contacts (white arrows) occur at 30-cm, 50-cm, and 34-cm depths in sites W02 (part A), W03 (part B), and W09 (part C), respectively. The TSL1 at 22–30-cm depth in W02 includes mud rip-ups and organic debris mixed with sand. The TSL1 at 45–50-cm depth in W03 shows a basal sand layer that fines upward into several sandy silt debris layers.

Table 5. *Summary of diatom results for Waatch Valley core sites.*

Core Site	Sample Depth (cm)	Sample Event Layer	Diatom Abundance on Slide	Diatom Trend Total Slide Count	Diatom Trend Scan Count
WA 02	25–28	TSL 1	Several	P–M (few O)	
WA 02	32–33	SUB1	Rare	P/M	
WA 03	45–48	TSL 1	Rare	P	
WA 03	52–56	SUB 1	Several	P (few M/O)	
WA 03	123–124	SUB 2	Many	P–M (few O)	
WA 03	137	Channel sand	None		
WA 03	162–163	Channel sand	Rare	P (one M?)	
WA 12	121–122	TDL 3	Abundant	P (several M/O)	
WA 12	125–126	TSL 3	Abundant	P/M/O	
WA 12	130–131	SUB 3	Abundant	O–M (several P)	
WA 12	135	"	Abundant	O/M (several P)	
WA 06	73	Mud	Abundant	P/M (many O)	M/P (several O)
WA 06	74	SUB 2a	Many	P/M (several O)	M–O (several P)
WA 06	106	Mud	Many	P–M (many O)	
WA 06	107	SUB 2b	Abundant	M–P (many O)	
WA 06	138	TDL 3	Abundant	P (few M/O)	P (few M, rare O)
WA 06	139	SUB 3	Abundant	M–P (several O)	M–P/O
WA 06	150	Channel sand	Abundant	P–M (several O)	

Key: P = polyhalobous, >30% salinity, includes "marine species"; M = mesohalobous, 0.2–30% salinity, includes "brackish species"; O = oligohalobous, <0.2% salinity, includes "freshwater species".
Dominance: X–YX is dominant; X/YX and Y are codominant.
Sample target events or event layers are listed 1–3.
Tsunami sand layers (TSL), tsunami debris layers (TDL), and presubsidence layers (SUB), or target horizons, are identified for each diatom sample.

accumulation of wetland mud and peat (Figure 6). Marine diatoms (polyhalobous) dominate in basal sand deposits at 162–163-cm depth in W03 and 150-cm depth in W06. The abundance of marine diatoms in the basal sand deposits indicates strong tidal flow associated with channel sand deposition in the upper Waatch Valley before wetland infilling (Table 5). Diatom trends are also analyzed from presubsidence marsh horizons to establish long-term trends of changing tidal flow in the Waatch Valley. Brackish diatom taxa dominate presubsidence wetland deposits at shallower depths of 139 cm in W06 and 130–131 cm in W12 in the upper reaches of the Waatch Valley. Marine diatoms dominate in presubsidence wetland deposits at much shallower depths of 32–33 cm in W02 and 52–56 cm in W03 in the lower Waatch Valley (Table 5). The lower reaches of the Waatch Valley maintained a strong tidal influence after the upper reaches of the Waatch Valley had become more brackish from wetland infilling and diminished tidal flow. Short-term marine inundations from cyclic marsh submergence and paleotsunami are superimposed on the long-term transition from lagoon to supratidal bog in the upper Waatch Valley, as shown below.

Paleotsunami Deposits

Anomalous sand layers are observed above the sharp upper contacts of subsidence events SUB1, SUB2a, SUB2b, and SUB3 in the lower Waatch Valley (Figure 6). Only the anomalous sand layer (TSL3), as observed directly above SUB3, is found to extend into the uppermost reaches of the Waatch Valley in W09, W11, and W12. Total slide counts of marine diatom abundance confirm marine surge inundation from relative increases in marine diatoms (polyhalobous) in paleotsunami deposit layers at depths of 25–28 cm (TSL1) in W02, of 45–50 cm (TSL1) in W03, of 129.5–130 cm (TSL3) in W12, and of 138 cm (TDL3) in W06 (Table 5). The association of marine surge inundation with coseismic subsidence confirms paleotsunami origins for the anomalous sand sheets. The increase in marine diatoms in the sandy organic-rich mud TDL3 above the subsidence contact SUB3 at 138–137-cm depth in W06 represents the maximum recorded marine inundation in the Waatch Valley, but its direct source is not certain, as it could reflect barrier ridge overtopping from the north (see further discussion below). For this reason the terminal TSL3 at W12 is used for the maximum inundation distance that is recorded in the Waatch Valley floodplain.

Paleotsunami sand layers range in thickness from 30 cm for TSL3 in W01 to 0.5 cm for TSL3 in W12 (Figure 6). The paleotsunami sand sheets generally decrease in thickness with distance upriver in the Waatch Valley. For example, TSL1 thickness is 14 cm in W14b, 20 cm in W01, and 9 cm in W02 in the lower Waatch Valley. The TSL1 layer decreases to only 5-cm thickness in W03 in the middle Waatch Valley (Figure 7). The TSL2 decreases in thickness from 19 cm in W03 to a 3-cm-thick sandy tsunami debris layer (TDL2b) above SUB2b at W13. The TSL3 has the greatest landward extent in the Waatch Valley, reaching W12 at a distance of 4.5 km from the present river mouth or tidal inlet (Table 2). The majority of paleotsunami sand layers demonstrate fining-up trends of sand grain size near the top of the sand layer. Two or more sand size fining-up layers are found in thick paleotsunami sand deposits in the lower Waatch Valley, such as in TSL2a in W01 and TSL2 in W03. This study focuses on maximum paleotsunami inundation in the upper reaches of the Waatch Valley where paleotsunami sand sheets are very thin, but are generally overlain by thicker silty debris layers (Figure 8).

Measured grain size distributions of sand fractions in representative paleotsunami sand layers in the Waatch Valley are presented in Table 6. Sample means range from 149 to 186 μm. Mean-normalized standard deviations range from 0.21 to

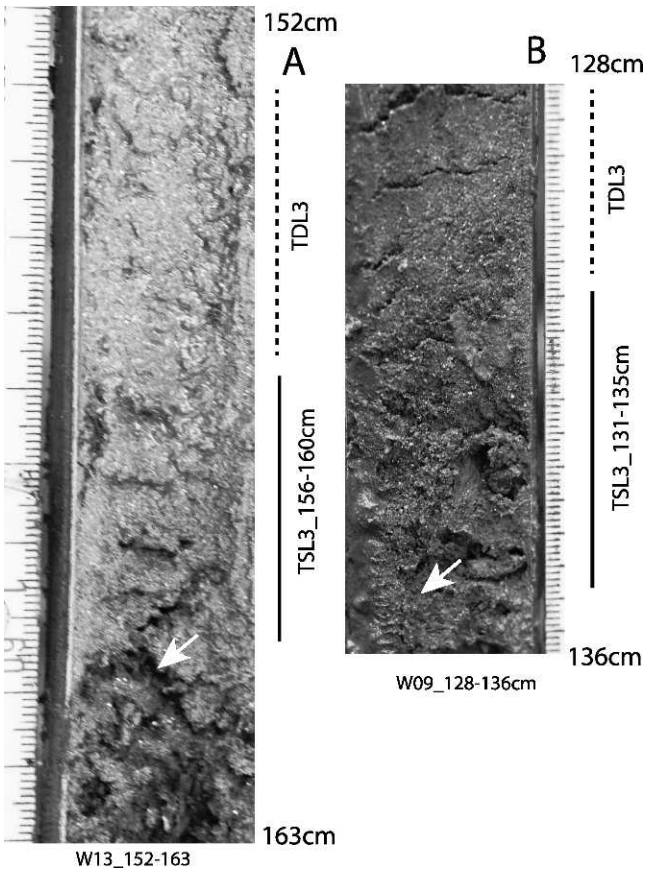

Figure 8. Photographs of thin paleotsunami sand layers in two core sites in the upper Waatch Valley. Fine silty sand (TSL3 solid line) occurs directly above subsidence horizons (white arrows) at 160-cm depth and 135-cm depth in sites W13 (part A) and W09 (part B), respectively.

0.42. Sand mean grain size does not decrease with landward transport distance in the Waatch floodplain as could be expected. Two possible factors could contribute to the lack of decreasing sand size with increasing transport distance in the Waatch Valley: (1) paleotsunami remobilization of Waatch Creek channel sand or (2) some sand is carried with coarse organic detritus in an advancing paleotsunami debris front.

Radiocarbon Dates

Radiocarbon dates constrain (1) the period of changing deposition from tidal lagoon to overlying vegetated wetlands in the Waatch Valley and (2) link Waatch subsidence and paleotsunami events to regional paleoseismicity in the North Central Cascadia Margin. The buried marsh radiocarbon samples are taken from *in situ* plant remains at the contact between the subsided marsh and overlying paleotsunami sand sheet or tsunami debris layer. These entombed *in situ* plant remains generally provide the best dates of coseismic subsidence. Paleotsunami deposits can include remobilized or "pre-event" organics and bulk peat horizons can also include organics accumulated over time before the subsidence event.

The earliest vegetated wetland deposit, developed by 1260–1330 (2-σ calibrated radiocarbon years BP), is in W12 in the upper reaches of the Waatch Valley (Table 7). Channel sand was still being deposited at 1060–1240 in W03 in the middle reaches of the Waatch Valley, demonstrating progressive down-valley infilling of the Waatch tidal lagoon. The lowest reaches of the Waatch Valley are expected to contain the shortest records of marsh development and hosted paleosubidence and associated paleotsunami records.

Radiocarbon dates of (1) 1260–1330 from the third subsidence event SUB3 at 135-cm depth in site W12 in the upper reaches of the Waatch Valley and (2) 920-1118 (middle date) from the second subsidence event(s) at about 90-cm depth in site WA–M from the middle Waatch Valley link the sequence of Waatch Valley subsidence events to regional megathrust ruptures (Table 7). Specifically, Waatch events SUB1, SUB2, and SUB3 are tentatively correlated to megathrust ruptures SUB-Y (AD 1700), SUB-W (1.1 ka), and SUB-U (1.3 ka) in the Central Cascadia Margin (Table 1). The observation of a second subsidence horizon SUB2a above SUB2b in the upper reaches of the Waatch Valley (Figure 6) represents the first apparent evidence of a potential megathrust rupture at this time period in the North Central Cascadia Margin (see further discussion below). In this study the number and sequence of subsidence events that are directly associated with paleotsunami inundations in the Waatch Valley during the last 1.3 ka are used to correlate the Waatch subsidence events to the regional record of megathrust ruptures. Many additional radiocarbon dates would be required to make these correlations on the basis of statistical analyses of radiocarbon age errors and age overlaps.

Neah Bay Back-Barrier Wetland Core Data

Seven representative core sites in the back-barrier wetlands of Neah Bay document episodic subsidence and associated paleotsunami overtopping of the barrier dune ridge (Figure 5). Core sites were partially determined by property ownership and avoidance of paleoliquefaction features, but they were primarily sited to test for barrier overtopping by paleotsunami (Schlichting and Peterson, 2006). The presence of sand dikes in back-barrier tsunami overtopping sites can lead to misinterpretation of paleotsunami sand layers in back-barrier settings in the Cascadia Margin, as is well documented in Cannon Beach, Oregon (Peterson *et al.,* 2008). Several cores at each paleotsunami overtopping site in the Neah Bay back-barrier wetlands were taken to assure that target paleotsunami sand layers were not locally emplaced by clastic sills or subaerial sand blows. This does not include liquefaction of paleotsunami sand layers, which can occur from subsequent earthquake events.

Core sites in the back-barrier wetlands are shore parallel and cross the Waatch Valley from west to east. The top of the Neah Bay barrier at site CEM01 (8 m NAVD88) is dated at 2170 $\pm$ 60 and 2070 $\pm$ 70 years BP (Table 7). Latest Holocene transgressive flooding of overwash or dune topography on the landward side of the Neah Bay barrier dune ridge resulted in variable depths (75–125 cm) of wetland peaty mud above basal sand deposits.

Table 6. *Grain size data for paleotsunami sand layers in the Waatch Valley and the Neah Bay back-barrier wetlands.*

Core Site	Event	Depth (cm)	Maximum (μm)	Minimum (μm)	Mean (μm)	Std.D.(μm)	Norm. Std.D.
Waatch							
W02	TSL1	22–25	274	98	169	37	0.21
W02	TSL1	25–28	352	98	186	41	0.22
W02	TSL1	28–31	372	78	183	50	0.27
W03	TSL1	47–48	352	98	183	45	0.25
W03	TSL1	49–50	431	98	186	49	0.26
W13	TSL3	153–160	372	59	149	44	0.29
W11	TSL3	120–122	274	78	169	58	0.34
W12	TDL3	121–122	313	78	164	58	0.35
W12	TDL3	125–126	274	59	155	41	0.26
W12	TSL	129–130	294	78	159	46	0.29
W06	TDL3	135–138	568	59	182	77	0.42
Neah Bay							
N08b	TSL3	131–131.5	490	80	208	82	0.39
N17	TDL1	28.5	310	50	146	54	0.37
N17	TSL2	44	430	90	171	63	0.37
N18	TSL1	35–38	510	90	216	64	0.29
N20	TDL1	51–53	330	60	159	51	0.32
N20	TSL2a	67–68	350	70	216	63	0.29
N20	TSL2b	73–75	410	60	226	73	0.32
N19	TSL2b	61–62	350	60	201	67	0.33
N19	TSL3	94–96	370	110	208	50	0.24

Sand fraction (0.062–2.0 mm) grain size intermediate diameters in micrometers.
Depth (cm) is below the surface level.
Sample means, standard deviation (Std.D.), and mean-normalized standard deviation (Norm. Std.D.) are all based on $N = 100$ grain counts.

Four shallow subsidence events each are recorded at sites N08b and N19 (Figure 9). Four radiocarbon samples are analyzed for the back–barrier sites (Table 7). One date is postmodern in site N18. It is discounted because of likely contamination from descending roots in the shallow barrier ridge deposit. The other three dates are from site N19 and include dates for SUB1 at 570–680, SUB2b at 1060–1260, and a submerged peaty soil developed on barrier sand (2.2 m NAVD88) at 2340–2430.

The shallow subsidence events SUB1–3 in the back-barrier sites are correlated to subsidence records in the upper Waatch Valley on the basis of the number and sequence of events that are associated with paleotsunami deposits in the upper 1.25-m core sections. Radiocarbon dates from N19 including SUB1

Table 7. *Radiocarbon dates from the Waatch Valley and Neah Bay back-barrier wetlands.*

Locality Core Site	Depth (cm)	Event	adjC14 adjRCYBP	Cal RC 1–σ calRCYBP	Cal RC 2–σ calRCYBP	Lab Beta #
Waatch						
W03	137	Channel	1260 ± 30	1070–1180	1060–1240	B291248
WA–M	80	SUB2	850 ± 130	681–908	556–1051	RIDDL370
WA–M	80		1100 ± 110	926–1178	795–1263	RIDDL369
WA–M	90		1080 ± 80	920–1118	795–1178	USGS2372
WA–M	90		1170 ± 130	963–1241	894–1310	RIDDL368
W12	135	SUB3	1360 ± 40	1280–1300	1260–1330	
Neah B.						
CEM01			2170 ± 60	2070–2307	2005–2330	Wessen
CEM01			2070 ± 70	1949–2125	1876–2303	Wessen
N18	39	SUB1	105.4 pMC			
N19	47	SUB1	700 ± 30	660–670	570–680	B311491
N19	62	SUB2b	1220 ± 30	1080–1220	1060–1260	B311492
N19	128	Barrier	2360 ± 30	2350–2360	2340–2430	B311493

Radiocarbon samples include *in situ* plant leaves and stems that were taken from the contact between peaty mud and overlying tsunami sand layers (TSL). One sample from 137-cm depth in W03 is taken from a channel sand deposit to establish the transition from tidal lagoon deposition to vegetated wetland deposition in the middle reaches of the Waatch Valley. Radiocarbon dates from SUB2 in WA–M in the Waatch Valley were taken from organic materials collected between 80- and 90-cm depth by Atwater (1992).
Radiocarbon dates include adjusted (adj) radiocarbon years before present, calibrated radiocarbon (at 1σ and 2σ analytic uncertainty), and the laboratory sample number (Beta Analytic Inc) or previously analyzed dates reported by Atwater (1992) for WA–M or by Gary Wesson (G. Wessen, pers. comm., 2010) for CEM01. Calibrations of previously reported dates are based on CALIB 6.0html (Stuiver, Reimer and Reimer, 2011).
Core site positions are shown in Figure 5 and summarized logs are shown in Figures 6 and 9.

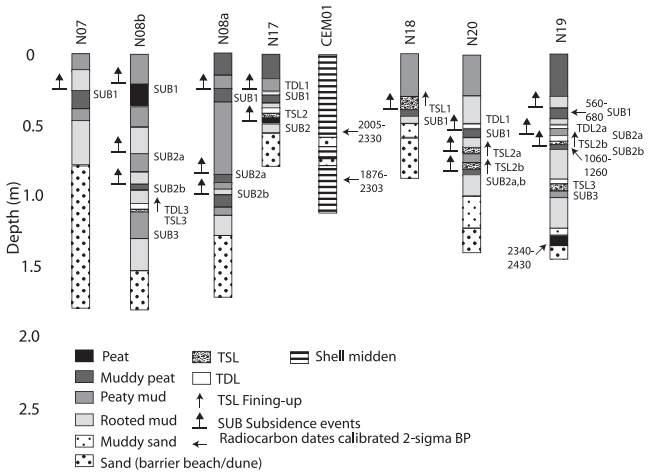

Figure 9. Summarized core logs from the Neah Bay back-barrier wetlands, generally ordered in two N-to-S traverses located at the west (N07–N17) and east (N18, N19) ends of the beach barrier dune ridge. Paleosubsidence (SUB) contacts are locally overlain by paleotsunami sand layers (TSL) or paleotsunami debris layers (TDL). See Figure 5 for core site positions in the back-barrier wetlands.

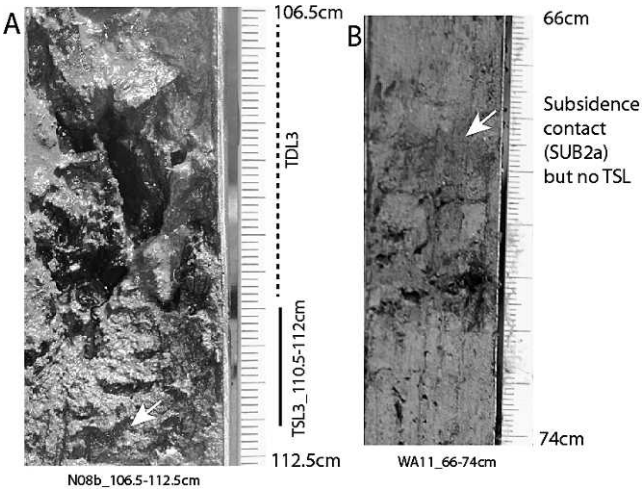

Figure 10. Photographs of subsidence horizons (white arrows) and paleotsunami sand layer (TSL3 solid line) for the Cascadia earthquake event SUB3 in N08b (part A) and a buried soil (SUB2a) from core site WA11. No paleotsunami sand layers or apparent paleotsunami debris layers were found at the sharp upper contact of the SUB2a subsided soil in site WA11. Core sites and core logs are shown in Figures 5 and 9, respectively.

(560–680) and SUB2b (1060–1260) are consistent with four subsidence events during the last 1500 years (Figure 6). An apparent subsidence event (SUB2a) in the region is shown for site WA11 in Figure 10. Submergence of the back-barrier wetlands at site N19 postdated a rooted soil (2340–2430) that developed directly on barrier sand deposits.

Anomalous sand layers in the back-barrier wetlands could only originate from marine surge overtopping of the barrier ridge, as the Waatch Creek both enters and flows south of the back-barrier wetlands (Figure 5). An abundance of monocrystalline quartz and feldspar grains, and the rare presence of rounded pyroxene and amphibole grains, in the sand layers confirm beach sand sources of TSL2a and TSL2b in N20, and TSL3 in N19. Eolian-transported sand grains are present in proximal back-barrier sites but they are rare in abundance and are highly disseminated in the muddy peat horizons. The direct correspondence between cyclic wetland subsidence and paleotsunami sand layer deposition ties the barrier overtopping surges to Cascadia paleotsunamis propagating eastward into the Juan de Fuca Strait (Figure 2).

A thin paleotsunami sand layer (TSL3) occurs above the SUB3 contact at 112-cm depth in N08b at the west end of the Neah Bay barrier (Figures 9 and 10). A coarse organic debris layer overlies the tsunami sand, likely representing woody detritus remobilized from the barrier ridge or back-barrier wetlands by the overtopping paleotsunami surge(s).

A very thin paleotsunami sand layer (0.5 cm in thickness) occurs above the second apparent subsidence horizon (SUB2) and below a thicker TDL2 at 42–43.5 cm depth in N17. A weak paleotsunami debris layer (TDL1) occurs directly above the first subsidence horizon (SUB1) in N17. The TDL1 contains disseminated sand and well-rounded lithic granules (3–5-mm diameter) mixed in with the detrital organics.

The record of paleotsunami overtopping is better developed at the east end of the Neah Bay barrier ridge where (1) TSL2a and TSL2b are preserved in site N20 and (2) TSL3 is of substantial thickness (5 cm) in N19 (Figures 9–11).

The barrier-overtopping sand sheets TSL2a and TSL2b do not extend widely in the back-barrier wetlands, indicating relatively short transport distances directed landward of the narrow Neah Bay barrier ridge. Although the last Cascadia paleotsunami at AD 1700 (Atwater *et al.,* 2005) did not leave tsunami sand layers in the more distal back-barrier sites N20 and N19, it did leave a substantial sand layer (TSL1) of several centimeters thickness in N18, located just landward of the barrier ridge crest (Figure 11).

DISCUSSION

Terminal Infilling of the Waatch Valley Lagoon

The records of coseismic subsidence and associated paleotsunami inundation, as correlated between core sites in the Waatch Valley and Neah Bay back-barrier wetlands, are short, reaching back less than about 1500 years (Figures 6 and 9). Net sedimentation in the upper Waatch Valley, about 1.5 m in 1300 years (Figure 6), coincides with measured relative sea level rise of about 1 mm y^{-1} for the last 2000 years in Discovery Bay marshes in the northern Olympic Peninsula (Williams, Hutchinson, and Nelson, 2005). There does not appear to be measureable evidence of net coastal uplift during the 1.3–0 ka period of infilling of the Waatch Valley. One previous study has reported ancient coastal uplift records at the Cape Flattery study area (Bird and Schwartz , 2000) but postglacial isostatic rebound appears to have terminated within the last 1300 years

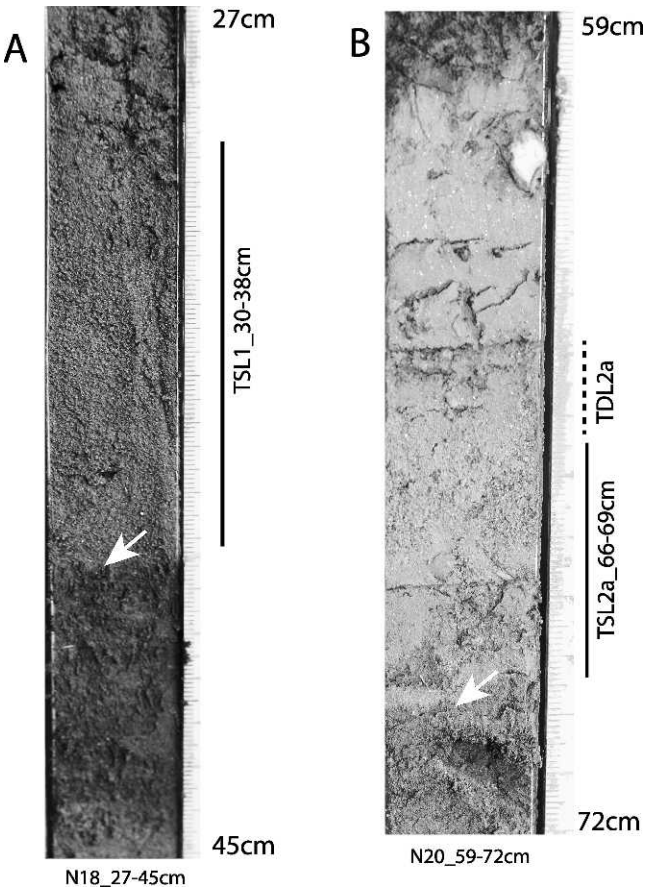

Figure 11. Photos of paleotsunami sand layers (solid line) above subsidence contacts (white arrow) for the last Cascadia earthquake at AD 1700 in site N18 (part A) and for the newly reported Cascadia earthquake at 0.7–0.9 ka in site N20 (part B). The TSL2a is partially sheared and liquefied, reflecting seismic shaking from the subsequent earthquake (SUB1) at AD 1700 (Table 1).

in the Waatch Valley, as is reported for the eastern Juan de Fuca Strait (Mosher and Hewitt, 2004).

One older peat date (2340–2430) at 2.2-m elevation in core site N19 from the Neah Bay back-barrier wetlands is intriguing. It is interpreted to represent a submerged rooted soil that developed on a protobarrier ridge between Neah Bay and the Waatch Valley. The Neah Bay barrier appears to have been in place by at least 2.3 ka. The conditions that initiated the transition from tidal lagoon to tidal marsh in the upper reaches of the Waatch Valley have not been established in this study. Deeper coring in the Waatch Valley deposits will be required to establish whether declining eustatic sea level rise, coastal uplift, or accretion of the Neah Bay barrier ridge at the north end of the Waatch Valley initiated the terminal infilling of the Waatch Lagoon All three factors could be associated with very late stage uplift from postglacial isostatic rebound, apparently terminating in the last 1.0–1.5 ka.

Coseismic Subsidence Events

Four elastic tectonic strain events of interseismic uplift and coseismic subsidence are recorded in the deeper and older wetland core sites in the Waatch Valley and Neah Bay back-barrier wetlands (Figures 6 and 9). Three subsidence events including SUB1, SUB2b, and SUB3 correlate to known Cascadia megathrust ruptures at AD 1700, 1.1 ka, and 1.3 ka, respectively (Atwater *et al.,* 2004). The younger of the two closely spaced subsidence events, SUB2a, correlates to a regional paleotsunami event, approximately dated 0.7–0.9 ka, from localities as widely spread as Tofino (510–780) and Port Alberni (670–954) in the Northern Cascadia Margin (Table 1) to Cannon Beach (Peterson *et al*. 2008), Rockaway (Schlichting and Peterson, 2006), and Neskowin (Peterson *et al.,* 2010) in northern Oregon (Figure 1). The restricted distribution of TSL2a in the Northern Cascadia Margin and a lack of associated coseismic subsidence in northernmost Oregon led to two competing hypotheses for its origin including (1) a near-field paleotsunami from a partial rupture of the Northern Cascadia Margin or (2) a far-field paleotsunami from a subduction zone in the northernmost Pacific rim (Schlichting, 2000). The correspondence between abrupt marsh burial and associated paleotsunami deposition at sites W01, N20, and N19 in the Neah Bay study area suggests a near-field paleotsunami origin, hypothesis 1, for TSL2a. The along-margin extent of this Northern Cascadia Margin rupture, SUB2a, has yet to be established. Additional shallow coring investigations in Tofino, British Columbia, the Juan de Fuca Strait of British Columbia and Washington, and Copalis, Washington (Figure 1) are warranted to establish an along-margin extent of this possible northern Cascadia rupture.

Estimates of Coseismic Subsidence

Estimates of the magnitude of coastal subsidence in the Waatch Valley study area are based on up-core transitions or steps of macrofossil paleotidal indicators, as established on the basis of the measured vegetation–macrofossil gradients from colonizing marsh (about 1.5-m elevation, NAVD88) to spruce bog (about 3.3 m) (Table 2). The macrofossil paleotidal steps used here are (1) slightly rooted mud, (2) peaty mud, (3) muddy peat, and (4) peat or tree roots (Figure 6). An absence of apparent steps between indicators in a recovered core interval is taken to represent 0 ± 0.5-m subsidence. An abrupt up-core step from peat (step 4) to rooted mud (step 1) represents 1.5 ± 0.5-m subsidence. Generally, the subsidence estimates for all four events are between 0.5 and 1.0 m relative sea level change. To account for differences in site response to wetland submergence the subsidence proxies for multiple core sites are weight averaged to yield subsidence values for events SUB1–4. Weighted average subsidence values for the Waatch Valley are as follows: SUB1 = 0.4 m, SUB2a = 0.4 m, SUB2b = 0.6 m, and SUB3 = 0.6 m (Table 8). The episodic coseismic subsidence is superimposed on the net sea-level rise (about 1.0 mm y^{-1}) recorded in the Waatch Valley (Figure 12), thereby preserving the records of megathrust ruptures in the northern end of the North Central Cascadia Margin.

Table 8. Coseismic subsidence transitions between marcrofossil paleotidal indicators in the Waatch Valley core sites.

Event	0 Step	One Step	Two Steps	Three Steps	Mean
SUB1	2	4	1		0.4
SUB2a	2	5			0.4
SUB2b		6	2		0.6
SUB3		5	2		0.6

Transitions between rooted mud, peaty mud, muddy peat, and peat are tabulated from cores W01, W03, W13, W09, W11, W12, and W06 (Figure 6). Mean values are estimated from counts of weighted steps (0, 0.5, 1.0 and 1.5) divided by the number of horizons to yield weighted averages.

Paleotsunami Run-Up Estimates

Paleotsunami run-up in the Waatch Valley is measured by tsunami deposit elevation in meters NAVD88 and distance in kilometers from the present tidal inlet. Tsunami sand sheets are traced landward until the sand pinches out and only a sandy organic-rich debris layer (TDL) is recorded (Figure 13). The sand sheet best represents the maximum recorded run-up in low-gradient alluvial floodplain settings, though it can underestimate maximum flooding distance (Peterson *et al.,* 2010).

The sand sheet from the last Cascadia paleotsunami TSL1 at AD 1700 is traced to site W03 at a distance of 3.2 km (Figure 13; Table 9). The maximum recorded run-up of the paleotsunami associated with subsidence event SUB2b at about 1.1 ka is traced to the TDL2b in site W13 at a distance of 4.0 km. The sand sheet from the paleotsunami at 1.3 ka is traced to a terminal TSL3 of 0.5-cm thickness in W12 at a distance of 4.5 km, where it pinches out to a TDL3 in W06 at 4.6-km distance. Several hundred meters to the north, another TSL3 layer (1.5-cm thick) is observed in N08b (Figure 9). The TSL3 in N08b

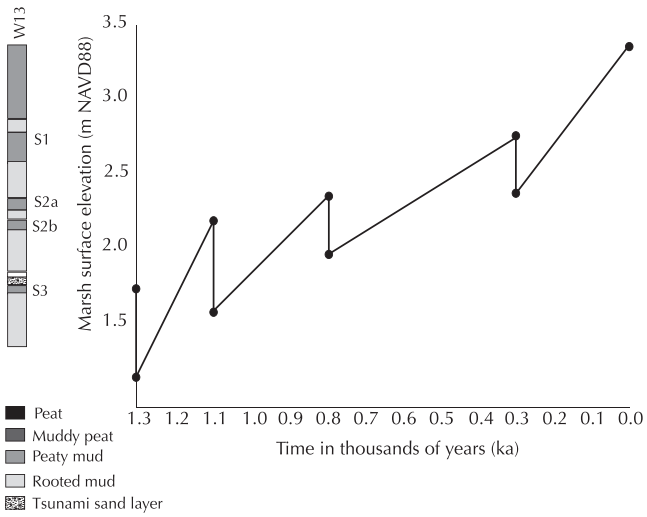

Figure 12. Plot of measured elevations of presubsidence marsh horizons or sea-level curve at site W13 (Table 2 and Figure 6) and weighted average of estimated coseismic subsidence (Table 8) for event ages SUB1 (0.3 ka), SUB2a (about 0.8 ka), SUB2b (1.1 ka), and SUB3 (1.3 ka) (Table 1). A slightly higher-than-expected modern elevation (3.3 m) at site W13 might reflect increased sediment supply following historic logging in the Waatch Valley drainages.

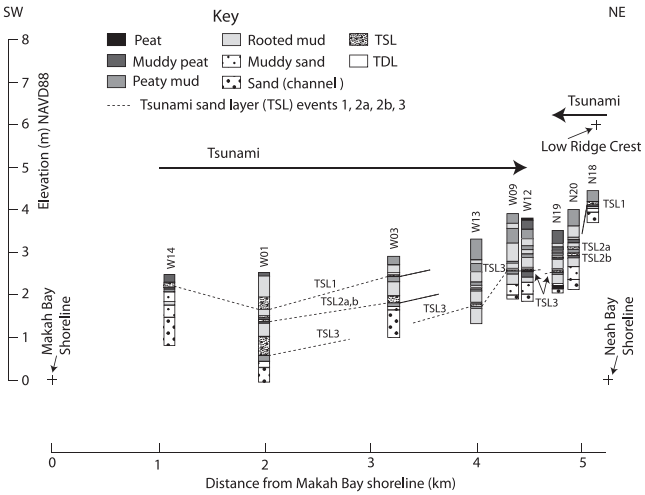

Figure 13. Plot of selected core logs relative to the NAVD88 elevation datum showing extent of paleotsunami sand layers (TSL1–3) in the Waatch floodplain (right arrow) or back-barrier wetlands (left arrow). The Neah Bay barrier ranges from 6- to 8-m elevation, with the low ridge crest shown in this plot. See Figure 5 for core site locations.

represents southward transport from paleotsunami overtopping of the Neah Bay barrier (see further discussion below).

The run-up heights of the paleotsunami at the ocean shoreline are estimated using (1) measured deposit elevation, (2) measured run-up distance, and (3) a run-up height attenuation of 3-m drop in run-up height per kilometer of inundation distance in the low-gradient Waatch floodplain (Table 9). This attenuation gradient was measured for the 1.3-ka paleotsunami in a similar alluvial floodplain setting, Beaver Creek, in central Oregon (Figure 1) (Peterson and Cruikshank, 2011).

To extrapolate the measured run-up in the Waatch Valley to an ocean shoreline run-up height the position of the paleoshoreline at the time of inundation must be established. The downvalley extents of tidal marshes and rooted sand flats in the lower Waatch Valley during the last millennium are mapped to sites W14a,b (Figures 5 and 6). Paleotsunami run-up height attenuation in the Waatch Valley floodplain is started from sites W14a,b at a distance of 1.3 km from the modern inlet shoreline. Extrapolated run-up heights at the W14 paleoshoreline are as follows: paleotsunami #1 at AD 1700 is 8.5 m NAVD88, paleotsunami #2b at 1.1 ka is 9.6 m, and paleotsunami #3 at 1.3 ka is 11.5 m (Table 9; Figure 14). These extrapolated run-up heights provide elevation targets for paleotsunami run-up investigations on the west coast of the Olympic Peninsula in northern Washington (Figure 2).

Paleotsunami overtopping of the Neah Bay barrier ridge crest (Table 9) provides limiting or minimum run-up heights for paleotsunamis at the entrance of the Juan de Fuca Strait. The barrier ridge ranges from 6-m elevation NAVD88 at its eastern end to 8 m at its western end, providing a range (6–8 m) of potential overtopping heights. A near-surface radiocarbon date (1876–2303) near the highest west end of the barrier ridge

Table 9. *Paleotsunami run-up elevations for the Waatch Valley and Neah Bay barrier overtopping.*

Core Site	Core Elev. (m)	Modern Shoreline Distance (km)	Paleovalley Distance (km)	Tsunami Deposit Event	Core Depth (m)	Deposit Elev. (m)	Shoreline Run-up Ht. (m)
Waatch							Extrap.
W14a,b	2.5	1.3	0	TSL1	0.17	2.3	
W01	2.5	2.0		TSL1	0.40	2.1	
W01	2.5			TSL2a	0.66	1.8	
W01	2.5			TSL2b	0.75	1.7	
W01	2.5			TSL3	1.03	1.5	
W03	2.9	3.2	2.0	TSL1	0.45	2.5	8.5
W03	2.9	3.2	2.0	TSL2	0.90	2.0	
W13	3.3	4.0	2.5	TSL2b	1.20	2.1	9.6
W13	3.3	4.0	2.5	TSL3	1.53	1.8	
W09	3.9	4.4		TSL3	1.27	2.6	
W11	3.8	4.5		TSL3	1.20	2.6	
W12	3.8	4.5	3.0	TSL3	1.25	2.5	11.5
W06*	3.8	4.6		TDL3	1.35	2.5	
Neah Bay							Barrier
N08b	4.5	–	0.4*	TSL3	1.09	3.4	>8
N17	4.5	–	0.4*	TDL1(?)	0.29	4.2	
N17	4.5	–	0.5*	TSL2	0.42	4.2	7–8
N18	4.5	–	0.2*	TSL1	0.30	4.2	6–7
N20	4.0	–	0.4*	TDL1	0.51	3.5	6–7
N20	4.0	–	0.4*	TSL2a	0.64	3.3	6–7
N20	4.0	–	0.4*	TSL2b	0.73	3.3	
N19	3.5	–	0.4*	TDL2a	0.53	3.0	
N19	3.5		0.4*	TSL2b	0.59	2.9	
N19	3.5		0.4*	TSL3	0.91	2.6	

Core site data: core top elevation (m NAVD88), upriver distance (km) from the modern beach shoreline at Makah Bay, and overland or paleovalley inundation distance (km) from the Hobuck Bridge (W14) (Figure 5). Back-barrier site overland distances (*) are measured from the present beach shoreline in Neah Bay.
Tsunami deposit: event (number), top of deposit (TDL if present, or TSL) in subsurface depth (m), and computed deposit elevation (m) relative to NAVD88 (site elevation data is from Table 2). Events are listed as tsunami sand layer (TSL) or tsunami debris layer (TDL) by number 1–3. Event#2 appears to be locally divided into two layers: above (a) and below (b).
Tsunami run-up height (m) based on deposit height and 3 m km^{-1} run-up height attenuation in the Waatch Valley floodplain (Figure 13), and adjacent barrier overtopping height in the Neah Bay back-barrier wetlands (Figure 15). Adjacent heights of the Neah Bay barrier ridge crest are 8 m, 7 m, and 6 m relative to sites N08b, N17, and N18, respectively. Sites N20 and N19 are landward of N18 so they share the same adjacent ridge crest height of 6 m NAVD88.

(site CEM01) predates the paleotsunami events TSL1–4 (0.3–1.3 ka) recorded in the back-barrier wetlands (Table 7).

The last Cascadia tsunami at AD 1700 overtopped the ridge crest at 6-m elevation NAVD88, adjacent to site N18 near the east end of the Neah Bay sand barrier (Figure 15). The AD 1700 paleotsunami did not leave a sand deposit at N17, which is located landward of a 7-m-elevation ridge crest. However, there is weak evidence of tsunami debris layer (TDL1) located above the SUB1 horizon in site N17. A thin paleotsunami sand layer (TSL2) is found above the second subsidence event (SUB2) at N17, but it is not present at N08b located directly landward of an 8-m NAVD88 barrier ridge crest. The paleotsunami associated with SUB3 at 1.3 ka did deposit a tsunami sand layer (TSL3) and an overlying sandy debris layer (TDL3) at site N08b. The 1.3-ka paleotsunami at Neah Bay exceeded 8 m NAVD88 in run-up height at the west end of the Neah Bay barrier ridge. If we assume about 1.0-m-deep overtopping surge and about 1.0-m-lower paleosea level at 1.3 ka, then the same flooding event today would reach about 10 m NAVD88 in the Neah Bay barrier ridge.

CONCLUSIONS

The unique position and geometry of the Waatch Valley coastal wetlands in northwest Washington provide important geologic records of cyclic coseismic subsidence and associated paleotsunami run-up. A Waatch Valley tidal lagoon likely bridged between Makah Bay on the exposed Pacific Ocean side and Neah Bay in the Juan de Fuca Strait before about 1.5 ka. The tidal lagoon progressively in-filled with peaty wetland mud, from north to south, during the last 1.3 ka. Four apparent events of coseismic subsidence are recorded in the Waatch Valley wetland deposits during the last 1.3 ka. The modest subsidence values (about 0.5–1.0 m) represent elastic strain cycles in the upper continental plate. Paleotsunami sand sheets that include ocean diatom taxa or beach sand grains (or both) are associated with all four recorded subsidence events during the last 1.3 ka. The evidence of paleotsunami excitation with each subsidence event indicates rapid megathrust ruptures, which correlate to regional great earthquakes in the North Central Cascadia Margin. Paleotsunami flooding of the Waatch wetlands occurred both by (1) long waves entering the Waatch Valley from the Pacific Ocean and (2) shorter wavelength surges overtopping the Neah Bay barrier ridge, located near the entrance of the Juan de Fuca Strait. The dated events of abrupt coastal subsidence and associated paleotsunami run-up in the Waatch Valley link previous reports of paleotsunami inundations in the study region to great subduction-zone earthquakes in the Northern Cascadia Margin.

ACKNOWLEDGMENTS

Tracy Handrich, Mary J. Robbins, William Nass, Dan Anderson, and J. Tait Elder provided assistance with coring,

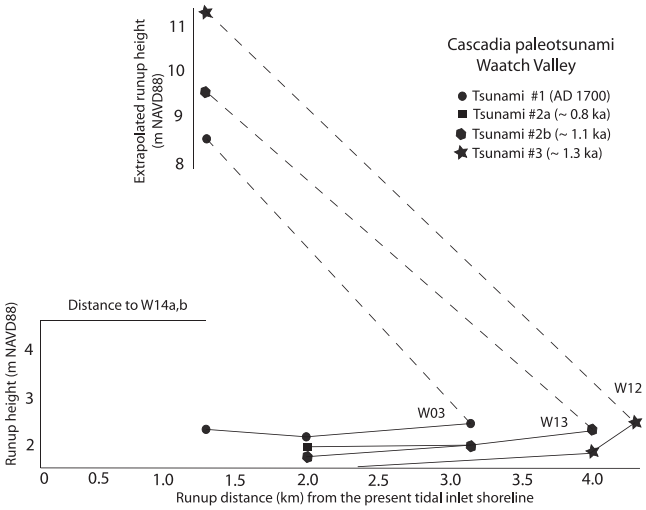

Figure 14. Measured paleotsunami run-up distances and heights (solid lines) and extrapolated run-up heights (dashed lines) taken to sites W14a,b, as based on measured paleotsunami attenuation of 3 m km^{-1} in a similar low-gradient alluvial valley, Beaver Creek, in the Central Cascadia Margin (Peterson and Cruikshank, 2011). Measured and extrapolated run-up data are from Table 9. Core site positions are shown in Figure 6.

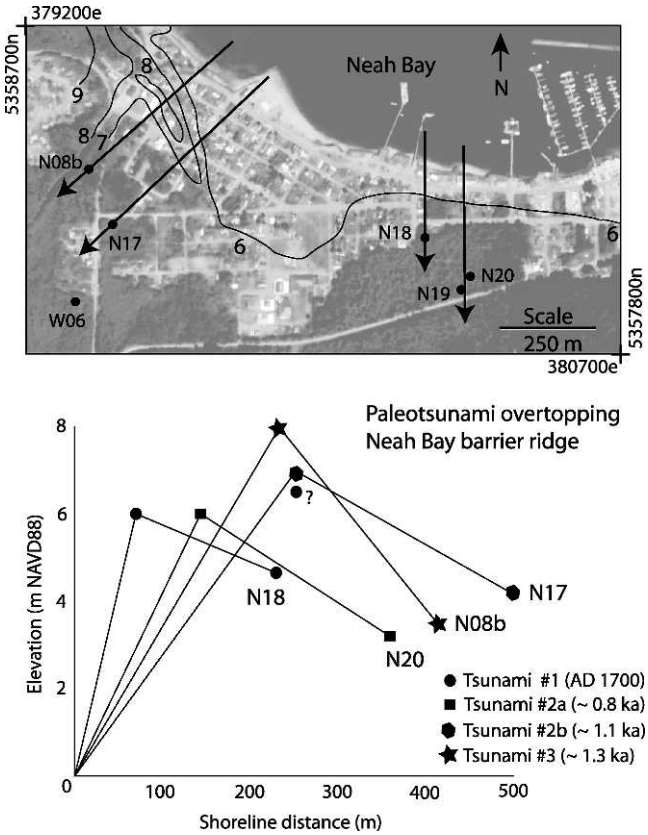

Figure 15. Barrier ridge overtopping heights in Neah Bay. Overtopping heights (minimum run-up) are taken from barrier ridge crest elevations (m NAVD88) that are closest to the shoreline (arrow trajectories) from dated paleotsunami deposits in back-barrier wetland sites (Table 9). Barrier ridge elevations are redrawn from Makah Indian Reservation (1970) and Makah Agency (1972). Background image is from Google Earth (2011).

core logging, and core photo archival in the Waatch and Neah Bay wetlands. Tracy Handrich performed microscopic grain size analyses of paleotsunami sand layers. Janine Bowechop, Makah Tribal Museum, provided logistical support for property access. Mark Armstrong, National Geodetic Survey NOAA, established GPS base station benchmarks for elevation control in the study area. Robert Steelquist, National Geodetic Survey NOAA, provided logistical support for the GPS base station surveying. Ray Colby, Makah Tribal Water Quality, provided modern salinity data for the Waatch River and Neah Bay back-barrier wetlands. Dave Herda, Makah Tribal geographic information system, provided topographic data for the Neah Bay barrier beach–dune ridge. Students in Geol 410/510 spring class, Portland State University, including Joshua Dinwiddie, Anthony Hofkamp, Shoshana Rosenberg, Katie Wojcik, and Dianna Woolsey, assisted with core site surveying and soil profiling in the Waatch Valley and Hobuck Beach plain. Brian Atwater provided reconnaissance study field notes, radiocarbon dates for site WA–M in the Waatch Valley wetlands, and suggestions for improvements to an early manuscript draft. Kennett Peterson provided editing assistance. The office of Research and Strategic Partnerships at Portland State University provided support for the radiocarbon dating that was performed for this investigation. We thank the Makah Tribal Council for permission to carry out this work.

LITERATURE CITED

Atwater, B.F., 1992. Geologic evidence for earthquakes during the past 2000 years along the Copalis River, southern coastal Washington. *Journal of Geophysical Research*, 97, 1901–1919.

Atwater, B.F.; Satoka, M.R.; Kenji, S.; Yoshinobu, T.; Kazue, U., and Yamaguchi, D.K., 2005. The orphan tsunami of 1700: Japanese clues to a parent earthquake in North America: U.S. Geological Survey, Professional Paper 1707, 133p.

Atwater, B.F.; Tuttle, M.P.; Schweig, E.S.; Rubin, C.M.; Yamaguchi, D.K., and Hemphill-Haley, E., 2004. Earthquake recurrence, inferred from paleoseismology. *In:* Gillespie, A.R.; Porter, S.C., and Atwater, B.F. (eds.), *The Quaternary Period in the United States*. Amsterdam, the Netherlands: Elsevier, pp. 331–350.

Bird, E. and Schwartz, M., 2000. Shore platforms at Cape Flattery, Washington. *Washington Geology* 28, 10–15.

Clague, J.J. and Brobowsky, P.T., 1994a. Evidence for a large earthquake and tsunami 100–400 years ago on the Western Vancouver Island, British Columbia. *Quaternary Research*, 41, 176–184.

Clague, J.J. and Bobrowsky, P.T., 1994b. Tsunami deposits beneath tidal marshes on Vancouver Island, British Columbia. *Geological Society of America Bulletin*, 106, 1293–1303.

Clague, J.J.; Bobrowsky, P.T., and Hutchinson, I., 2000. A review of geological records of large tsunamis at Vancouver Island, British Columbia, and implications for hazard. *Quaternary Science Reviews*, 19, 849–863.

Clague J.J.; Hutchinson, I.; Mathewes, R.W., and Patterson, R.T., 1999. Evidence for late Holocene tsunamis at Catala Lake, British Columbia. *Journal of Coastal Research*, 15, 45–60.

Darienzo, M.E., 1991. Late Holocene Paleoseismicity along the Northern Oregon Coast. Portland, Oregon: Portland State University, doctoral thesis, 167p.

Google Earth, 2011. Google Earth V 6.0. http://www.google.com/earth/ (accessed November 10, 2011).

Hemphill-Haley, E., 1993. Taxonomy of recent and fossil (Holocene) diatoms (Bacillariphyata) from northern Willapa Bay, Washington. U.G. Geological Survey Open File Report 93-289. 151p.

Jensen, N.G. and Hustedt, F., 1985. *The Pennate Diatoms, A Translation of Hustedt's "Die Kieselalgen". 2.* Koenigstein, Germany: Koeltz Scientic Books, 918p.

Makah Indian Reservation, 1970. Makah Indian Reservation Neah Bay Village, Neah Bay, Washington, Topography Map–1970. Scale 1″–100′, contours at 2′ intervals. Digital copy provided by D. Herda, Makah Tribal GIS services (2011).

Makah Agency, 1972. Neah Bay Village MIR 15–72 Topographic Map. Scale 1″–50′, contours at 2′ intervals. Jay Whiteford and Assoc. contract DOT–FHIO–2506, April 29, 1972. U.S. Department of Interior, Bureau of Indian Affairs.

Mosher, D.C. and Hewitt, A.T., 2004. Late Quaternary deglaciation and sea-level history of eastern Juan de Fuca Strait, Cascadia. *Quaternary International,* 121, 23–39.

Patrick, R. and Reimer, C.W., 1966. The diatoms of the United States, exclusive off Alaska and Hawaii, I. Philadelphia: *Monographs of Academy of Natural Sciences*, Volume 13, 688p.

Peterson, C.D. and Cruikshank, K.M., 2011. Proximal records of paleotsunami run-up in barrage creek floodplains from late-Holocene great earthquakes in the Central Cascadia Suduction Zone, Oregon, USA. *In:* Mokhtari, M. (ed.), *Tsunami—A Growing Disaster*. InTech, available from: http://www.intechopen.com/articles/show/title/proximal-records-of-paleotsunami-runup-in-barrage-creek-floodplains-from-late-holocene-great-earthquakes (accessed May 8, 2012).

Peterson, C.D.; Cruikshank, K.M.; Jol H.M., and Schilichting, R.B., 2008. Minimum runup heights of paleotsunami from evidence of sand ridge overtopping at Cannon Beach, Oregon, Central Cascadia Margin, USA. *Journal of Sedimentary Research*, 78, 390–409.

Peterson, C.D.; Cruikshank, K.M.; Schlichting, R.B., and Braunsten, S., 2010. Distal runup records of latest Holocene paleotsunami inundation in alluvial floodplains: Neskowin and Beaver Creek, Oregon, Central Cascadia Margin, USA. *Journal of Coastal Research*, 26, 622–634. doi 10.2112/08–1147.1

Schlichting, R.B., 2000. Establishing the Inundation Distance and Overtopping Height of Paleotsunami from Late-Holocene Geologic Records at Open Coastal Wetland Sites, Central Cascadia Margin. Portland, Oregon: Portland State University, Masters thesis, 166p.

Schlichting, R.B. and Peterson, C.D., 2006. Mapped overland distance of paleotsunami high-velocity inundation in back-barrier wetlands of the Central Cascadia Margin, USA. *Journal of Geology*, 114, 577–592.

Stuiver, M.; Reimer, P.J., and Reimer, R., 2011. CALIB radiocarbon calibration. Execute version 6.0html. http://calib.qub.ac.uk/calib/ (accessed January 26, 2011).

U.S. Geological Survey, 2011. Seamless Map Data: http://seamless.usgs.gov/ (accessed October 12, 2011).

Williams, H. and Hutchinson, I., 1998. Stratigraphic and microfossil evidence for late Holocene tsunamis at Swanton Marsh, Whidbey Island, Washington. *Quaternary Research*, 54, 218–227.

Williams, H.F.L.; Hutchinson, I., and Nelson, A.R., 2005. Multiple sources for late-Holocene tsunamis at Discovery Bay, Washington State, USA. *The Holocene,* 15, 60–73.

APPENDIX

Diatom species scan counts for selected samples.

Diatom species W06	73 cm	74 cm	138 cm	139 cm
Polyhalobous	95	33	127	31
Achanthes brevipes				
Actinoptychis senarius		1		
Amphora proteus				
Biddulphia dubia				
Cocconeis scutellum	9	1	27	1
Coscinodiscus radiatus	3			
Dephineis surirella				
Endictya sp.	8	4		4
Gramattophora oceanica				1
Hyalodiscus scoticus				
Paralia sulcata	66	27	100	24
Thalassiosira eccentrica				
Thalassiosira pacifica				
Trachyspenia australis	9			1
Mesohalobous	94	101	9	152
Biddulphia aurita				
Caloneis westii	7	1		
Cocconeis diminuta	42			
Cyclotella striata				
Diploneis didyma	1	18	3	39
Diploneis interrupta		4		
Diploneis pseudovalis		5		3
Gyrosigma eximium				1
Gyrosigma acumintium	2			
Navicula cincta				
Navicula lanceolata		1		
Navicula lyra				1
Navicula phyllepta	18	39	2	52
Nitzschia acuminata	7		1	2
Nitzschia fasciculata	5	23		48
Nitzschia granulata	1		2	
Nitzschia lanceola				
Nitzschia levidensis	2			
Nitzschia navicularis		1		
Pinnularia viridis		7	1	1
Rhopalodia gibbenula	5	1		2
Rhopalodia musculus				
Synedra fasciculata	4	1		3
Oligohalobous	35	49	1	37
Amphora libyca				
Diploneis ovalis				5
Epithemia turgida	2			
Eunotia pectinalis	4	1		6
Fragilleria constricta				
Gomphonema augustatum		1		5
Gomphonema parvulum		1		
Navicula mutica		5		5
Navicula pussilla	29	29	1	12
Navicula radiosa				
Pinnularia lagerstedi		12		3
Rhoicospenia curvara				
Surirella brebissonii				1
Tabellaria fenestrata				